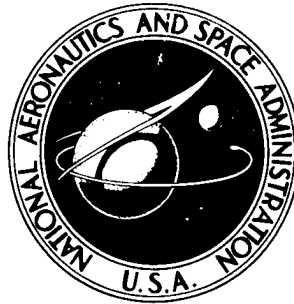


NASA TECHNICAL NOTE



NASA TN D-3022

NASA TN D-3022

**EVALUATION OF THE LATERAL-DIRECTIONAL
STABILITY AND CONTROL CHARACTERISTICS
OF THE LIGHTWEIGHT M2-F1
LIFTING BODY AT LOW SPEEDS**

by Harriet J. Smith

*Flight Research Center
Edwards, Calif.*

NASA TN D-3022

EVALUATION OF THE LATERAL-DIRECTIONAL STABILITY AND
CONTROL CHARACTERISTICS OF THE LIGHTWEIGHT M2-F1
LIFTING BODY AT LOW SPEEDS

By Harriet J. Smith

Flight Research Center
Edwards, Calif.

NATIONAL AERONAUTICS AND SPACE ADMINISTRATION

For sale by the Clearinghouse for Federal Scientific and Technical Information
Springfield, Virginia 22151 - Price \$2.00

EVALUATION OF THE LATERAL-DIRECTIONAL STABILITY AND CONTROL CHARACTERISTICS
OF THE LIGHTWEIGHT M2-F1 LIFTING BODY AT LOW SPEEDS

By Harriet J. Smith
Flight Research Center

SUMMARY

The lateral-directional stability and control characteristics of the lightweight M2-F1 lifting body were investigated during glide flights. Prior to flight testing, full-scale wind-tunnel data were used in both analytical and simulator studies to predict the handling qualities of the vehicle. For the glide tests, the vehicle was towed by a C-47 airplane to an altitude of approximately 12,000 feet (3,658 meters) and released. Sideslips, rudder-fixed aileron rolls, and aileron and rudder pulses were performed during the glides over a range of angle of attack from -3° to 13° (-0.05 to 0.22 rad) and at velocities from 77 knots to 119 knots (39.6 to 61.2 meters/second).

The M2-F1 configuration tested was found to be sluggish in roll as a result of the combination of high dihedral effect and adverse yaw produced by the ailerons. The high dihedral effect also caused the vehicle to be extremely sensitive to gusts. Based on previous standards for evaluating the handling qualities of piloted fighter-type aircraft, the M2-F1 controllability in roll would be considered marginal, primarily because the ailerons are not effective enough to counteract the disturbances caused by gusts. For the limited mission utilization of a reentry vehicle, however, the pilots considered the handling qualities of the vehicle to be adequate.

INTRODUCTION

With the increasing interest in space travel, considerable effort is being devoted to developing a reentry vehicle that would combine some of the design and operational simplicity of a capsule with the mission flexibility of a lifting vehicle. In support of this effort, the National Aeronautics and Space Administration is investigating several lifting-body shapes.

To realize fully the advantages that are to be gained from the lifting capability of a vehicle, the vehicle must be capable of being maneuvered, especially during entry and landing. Therefore, the stability and control characteristics are important in the development of lifting reentry vehicles. Although much can be learned from wind-tunnel and simulator studies, only through actual flight testing can this new class of vehicles be adequately evaluated. For this purpose, a lightweight glide vehicle was built for

testing at the NASA Flight Research Center, Edwards, Calif., to assess handling qualities and performance. The M2-F1 configuration was chosen for the tests primarily because of the availability of extensive wind-tunnel data at the start of the program. Since this flight vehicle was the first of its type, full-scale wind-tunnel tests were deemed advisable. Consequently, the flight vehicle was tested in the 40- by 80-foot tunnel at the NASA Ames Research Center prior to the flight tests.

After some initial flights for pilot familiarization, in which the vehicle was towed by an auto, the M2-F1 was towed by a C-47 airplane to an altitude of about 12,000 feet (3,658 meters). After release, stability and control data were obtained during the glide portion of the flight, which covered a velocity range from 77 knots to 119 knots (39.6 to 61.2 meters/second) and an angle-of-attack range from -3° to 13° (-0.05 to 0.22 rad). This paper summarizes the lateral-directional stability and control characteristics investigated during the flight tests and compares some wind-tunnel data with the flight values. Performance data from the tests are reported in reference 1.

SYMBOLS

The units used for the physical quantities in this paper are given both in the U.S. Customary Units and in the International System of Units (SI). Factors relating the two systems are given in reference 2.

| | |
|----------|---|
| a_y | transverse acceleration, g |
| b | body span, feet (meters) |
| C_l | rolling-moment coefficient, positive right |
| C_n | yawing-moment coefficient, positive right |
| C_y | lateral-force coefficient, positive right |
| g | acceleration due to gravity, feet/second ² (meters/second ²) |
| I_x | moment of inertia about longitudinal axis, slug-foot ² (kilogram-meter ²) |
| I_y | moment of inertia about lateral axis, slug-foot ² (kilogram-meter ²) |
| I_z | moment of inertia about normal axis, slug-foot ² (kilogram-meter ²) |
| I_{xz} | product of inertia, slug-foot ² (kilogram-meter ²) |
| P | period, seconds |
| p | rolling angular velocity, radians/second |

| | |
|-----------------|--|
| q | pitching angular velocity, radians/second |
| \bar{q} | dynamic pressure, pounds/foot ² (newtons/meter ²) |
| r | yawing angular velocity, radians/second |
| S | planform area, foot ² (meter ²) |
| t | time, seconds |
| V | true airspeed, knots (meters/second) |
| W | weight, pounds (kilograms) |
| α | angle of attack, degrees (radians) |
| α_0 | angle of attack with respect to the principal axis, degrees (radians) |
| β | angle of sideslip, degrees (radians) |
| δ | control-surface deflection, degrees (radians) |
| δ_a | lateral-control deflection, $\delta_{\text{left}} - \delta_{\text{right}}$, degrees (radians) |
| δ_e | elevon deflection, positive trailing edge down, degrees (radians) |
| δ_f | trailing-edge-flap deflection, positive trailing edge down, degrees (radians) |
| δ_r | rudder deflection, positive trailing edge left, degrees (radians) |
| ζ | damping ratio |
| ϕ | bank angle, degrees (radians) |
| ω_ϕ^2 | numerator of the transfer function for control of roll rate |
| ω_ψ^2 | static-stability parameter for the short-period (Dutch roll) lateral-directional mode |

$$C_{l\beta} = \frac{dC_l}{d\beta} \text{ per radian}$$

$$C_{l\delta_a} = \frac{dC_l}{d\delta_a} \text{ per radian}$$

$$C_{l\delta_r} = \frac{dC_l}{d\delta_r} \text{ per radian}$$

$$C_{n\beta} = \frac{dC_n}{d\beta} \text{ per radian}$$

$$C_{n\delta_a} = \frac{dC_n}{d\delta_a} \text{ per radian}$$

$$C_{n\delta_r} = \frac{dC_n}{d\delta_r} \text{ per radian}$$

$$C_{Y\beta} = \frac{dC_Y}{d\beta} \text{ per radian}$$

$$C_{Y\delta_a} = \frac{dC_Y}{d\delta_a} \text{ per radian}$$

$$C_{Y\delta_r} = \frac{dC_Y}{d\delta_r} \text{ per radian}$$

$$L_\beta = \frac{\dot{q}SbC_{l\beta}}{I_X} \text{ per second}^2$$

$$N_\beta = \frac{\dot{q}SbC_{n\beta}}{I_Z} \text{ per second}^2$$

$$L_{\delta_a} = \frac{\dot{q}SbC_{l\delta_a}}{I_X} \text{ per second}^2$$

$$N_{\delta_a} = \frac{\dot{q}SbC_{n\delta_a}}{I_Z} \text{ per second}^2$$

A dot above a symbol denotes differentiation with respect to time.

DESCRIPTION OF VEHICLE

The M2-F1 lifting body is basically a blunt 13° (0.22 rad) half-cone with a tapered afterbody (refs. 3 to 9). Pertinent geometric characteristics are given in table I, and a three-view drawing is shown in figure 1. The vehicle is unpowered and is towed to altitude and released for flight testing. A small solid-propellant rocket provides assistance at landing, when necessary.

The hull of the lightweight M2-F1 vehicle was constructed of 3/32-inch (0.2 centimeter) mahogany plywood and the frame of welded steel tubing. The

main-gear shock and strut units incorporate a viscous damper and bungee combination. The main-wheel and nose-gear assemblies are modified light-aircraft units. The vertical fins, rudders, and elevons were constructed of aluminum sheet and the trailing-edge flaps of aluminum tubing, covered with a synthetic fabric. A more detailed description of the vehicle is presented in reference 1, and a photograph is shown in figure 2.

At the time the vehicle was constructed, a detailed breakdown of the mass distribution was made and the moments of inertia were calculated. These inertias, which were for an 840-pound vehicle (381 kilograms), are given in table I. Most of the preliminary analysis was based on this weight. Subsequently, instrumentation, an ejection seat, and a small solid-propellant landing-assist rocket were added, resulting in a vehicle weight of 1182 pounds (536.2 kilograms). The contribution of these added items to the moments of inertia were estimated, and the resulting values are given also in table I. These values were used in the determination of the derivatives from flight data.

During this investigation, three control systems were considered. Schematic drawings of the systems are shown in figure 3. In the scheme illustrated in figure 3(a), both the trailing-edge surfaces (flaps) and the outboard surfaces (elevons) were connected to the control stick and used together for lateral control. The second scheme (fig. 3(b)) utilized only the outboard elevons for lateral control. In both of these schemes, longitudinal control was obtained from both pairs of surfaces, and both rudder surfaces were connected to foot pedals in a conventional manner for directional control. For clarity, the rudder system was omitted from the drawings. The control scheme illustrated in figure 3(c) is unconventional in that the rudders were connected to the control stick and were used as the primary roll control. Both the trailing-edge flaps and the outboard elevons were connected to the foot pedals and were used for directional control. Longitudinal control was achieved, as before, with both elevons and flaps.

The flight tests discussed herein were made using the control scheme illustrated in figure 3(b) in which only the elevons were used for lateral control.

INSTRUMENTATION

Quantities pertinent to this investigation were measured with standard NASA instrumentation. A common timer was used to synchronize the internal records. An airspeed head mounted on a nose boom approximately $4\frac{1}{2}$ feet (1.37 meters) long measured both total and static pressure. The airspeed was calibrated by a pacer aircraft and is believed to be accurate to within ± 1 knot (± 0.5 meter/second).

Angles of attack and sideslip were measured by vanes mounted on the nose boom and recorded on a 12-channel oscillograph. Both quantities were calibrated in the Ames 40- by 80-foot wind tunnel. The angle of attack was also

calibrated in flight, which confirmed the wind-tunnel calibration. In addition, corrections were made for angular velocities for both angle of sideslip and angle of attack. The overall accuracy of these quantities for this investigation was approximately $\pm 1^\circ$ (± 0.02 rad).

The approximate errors in the other quantities within the range where data were obtained were:

$$\delta_r = \pm 0.5^\circ (\pm 0.01 \text{ rad})$$

$$\delta_f = \pm 0.5^\circ (\pm 0.01 \text{ rad})$$

$$\delta_e = \pm 2.0^\circ (\pm 0.03 \text{ rad})$$

$$q = \pm 0.02 \text{ rad/sec}$$

$$r = \pm 0.02 \text{ rad/sec}$$

$$p = \pm 0.04 \text{ rad/sec}$$

$$a_y = \pm 0.05g$$

PRELIMINARY ANALYSIS

Prior to the flight-test program, the M2-F1 was tested in the Ames 40- by 80-foot wind tunnel over an angle-of-attack range from 0° to 22° (0.38 rad) at airspeeds of 57 knots, 70 knots, and 85 knots (29.3, 37, and 43.7 m/sec). Data were obtained with the center fin and the elevons both on and off. The results are shown in figures 4(a) to 4(c). Figure 4(a) shows the full-scale aileron derivatives for two control configurations with the center fin off. The elevon-only data were obtained by subtracting the elevon-off data from the data obtained with both the flaps and the elevons and, hence, are only approximate. The effect of the center fin is shown for the configuration with both flaps and elevons. Rudder derivatives and sideslip derivatives obtained with the center fin on and the center fin off are shown in figures 4(b) and 4(c), respectively. For comparison, small-scale data obtained on a 37-inch model (0.9 meter) are also included in all three figures for the center-fin-on configuration with both flaps and elevons used for ailerons.

It was discovered later that the instrumentation used in the full-scale tests was not accurate enough to obtain reliable data at low dynamic pressures. Errors as large as 50 percent were determined for the side-force measurements and, since side force enters into the rolling- and yawing-moment calculations, these values would also be affected. However, the basic stability data shown in figure 4 agree fairly well with previous small-scale-model data. Conversely, considerable differences are noted in the control derivatives, but it is not certain how much of the discrepancy should be attributed to wind-tunnel error and how much to differences between the models and the actual vehicle.

Thus, the data were used without correction for the preliminary preflight analytical and simulator studies of the handling qualities needed to plan and conduct the flight program.

Center Fin

Because the available data indicated that the stability of the M2-F1 would be marginal, a large center fin was provided to increase the directional stability. Because of the operational problems that might be encountered in future vehicle applications, preliminary studies were directed toward finding a suitable configuration with the center fin removed. Wind-tunnel tests were conducted, therefore, both with and without the center fin. Computed Dutch roll periods and damping ratios for the two configurations are shown in figure 5. Although the vehicle is stable without the center fin, the damping is less in this configuration. Thus, the first ground tow tests were made in the fin-on configuration.

Control Response

One of the problems encountered in the early studies was that of obtaining adequate roll control. Several control schemes were investigated on the simulator in an attempt to find a practical solution; three of the schemes were described on page 5. Time histories of the responses to lateral control-stick step inputs are shown in figures 6(a) to 6(c) for the three control systems illustrated in figures 3(a) to 3(c), respectively. In the first time history (fig. 6(a)), the roll-control input produced an adverse yawing moment which, because of the large dihedral effect, resulted in a very sluggish lateral-control response. The response from the outboard surfaces only is shown in figure 6(b). From an examination of the derivatives shown in figure 4, it can be seen that, although the rolling moment due to aileron is approximately one-half that when both surfaces are used, the yawing moment is essentially eliminated. The result, as shown, is a net increase in roll response.

During early simulator studies of various control combinations, it was observed that the rudders, due to the large dihedral effect of the vehicle, acted as a powerful roll control. Whereas, with the ailerons this large dihedral effect plus negative $C_{n\delta_a}$ were cause for a sluggish roll-control

system, with the rudder, the ratio $\frac{C_{n\delta_r}}{C_{l\delta_r}}$ was large enough to cause a rapid

roll reversal. This phenomenon is illustrated in figure 6(c). A slight delay occurs just before the reversal, but on the simulator the delay was barely noticeable to the pilots. The pilots preferred to use the rudders as the primary roll control. The first flight tests, therefore, were made with the rudders connected to the control stick for roll control. The four aileron surfaces appeared to provide an acceptable yaw control and, thus, were connected to the pedals.

Characteristics of the Vehicle on Tow

Experience with vehicles on tow had indicated that towing the M2-F1 might pose serious problems. Therefore, both analytical and simulator studies included an investigation of the stability and control characteristics of the vehicle on tow. Unlike most vehicles which are less stable on tow than in free flight, the M2-F1 was predicted to be more stable when being towed.

TESTS

Car Tows

Flight testing of the lightweight M2-F1 with the center fin installed began with a series of car tows to familiarize the pilot with the vehicle's overall handling qualities. The vehicle was not instrumented for these first tests. The first few attempts to fly were unsuccessful, primarily because of the turbulence created by the tow car. The vehicle bounced from side to side and was rarely airborne for more than a second. The pilot reported that the vehicle appeared to be unstable in the Dutch roll mode, contrary to the results of both the analytical and the simulator studies. Movies were taken of the flights, and examination of the vehicle motions on a data analyzer revealed that the oscillations were sustained by pilot input and contact of the landing gear with the ground. The control-system hookup (rudder surfaces for roll) contributed to the piloting problem because of the initial acceleration in the opposite direction. Although this initial opposite acceleration was evident in the simulator outputs, the pilot did not believe it to be serious. Inasmuch as a fixed-base simulator was used for this study, the pilot did not feel the acceleration but observed it only as a slight lag before rolling in the proper direction. However, this initial opposite roll acceleration when perceived visually and through motion cues in proximity to the ground caused the pilot to overcontrol.

The controls were then connected in a more conventional manner, using only the outboard surfaces for lateral control. The first attempt to fly this configuration was also unsatisfactory because of an apparently unstable Dutch roll mode. In an attempt to find a configuration that would fly, the center fin was removed. Although this change was predicted to make the vehicle less stable, it appeared to the pilot to solve the problem. This successful flight was made in the early morning with no wind. The previous attempts to lift off were made on hot summer afternoons, with little regard for thermal heating or wind. Because this test demonstrated that the vehicle could be flown without the center fin and because one of the initial aims was the removal of this fin, the flight-test program was continued without the fin.

Glide Tests

After the initial car tows, the M2-F1 without the center fin was towed by a C-47 airplane to an altitude of approximately 12,000 feet (3,658 meters) and

released. The tests discussed herein were performed during the ensuing free-flight and consisted of steady sideslips, rudder-fixed aileron rolls, aileron pulses, and rudder pulses. The elevons were used for lateral control (see fig. 3(b)). Data were obtained over an angle-of-attack range from -3° to 13° (-0.052 to 0.227 radian) and a velocity range from 77 knots to 119 knots (39.6 to 61.2 meters/second). Time histories of some typical maneuvers are shown in figures 7 to 10. Figures 7 and 8 show the responses to an aileron and a rudder pulse, respectively, which illustrate the large roll-to-yaw ratios obtained. Data from a rudder-fixed aileron roll are presented in figure 9. As shown, the roll due to yaw counteracted the roll from the ailerons. The combination of large dihedral and adverse yaw from the ailerons limits the roll rates which can be obtained from the ailerons. These effects are again illustrated in figure 10 in the data from a steady-sideslip maneuver in which a small rudder input required relatively large aileron inputs to maintain the steady sideslip.

RESULTS AND DISCUSSION

Because the test vehicle was unpowered and had a low lift-drag ratio, the duration of the flights was necessarily short and the test periods limited. Also, the simple, flexible control system used on the vehicle made it nearly impossible for the pilot to keep the ailerons fixed. Consequently, the quality of the data, as illustrated in some of the time histories, was relatively poor for analysis purposes, and many of the results presented herein are considered more qualitative than quantitative.

Gust Response

During early car-tow tests, a disturbing vehicle response to mild wind shears and tow-vehicle turbulence was noted. Because of the large dihedral of the vehicle, almost imperceptible sideslip angles or light turbulence caused rapid roll rates. Moderate bank angles were obtained before the pilot could successfully counteract the motion. When this motion occurred close to the ground, it tended to cause the pilot to overcontrol and induce an oscillation. In free-flight the vehicle was even more sensitive to gusts than it was on tow, because of the absence of the directional-stability increment provided by the towline.

As the pilot gained experience, he was able to maintain control of the vehicle by riding out the initial perturbation, since it was not divergent. When the roll rate reached zero, he returned the vehicle to a level attitude.

Dutch Roll Damping and Frequency

The pilot's comments after the first successful air tow were generally favorable concerning vehicle stability both on and off tow. He reported the frequency and the damping of the Dutch roll mode to be higher than predicted.

The flight data for this mode are shown in figure 11. Although there is considerable scatter in the data, the results generally confirm the pilot's observations. The pilot also reported that, because of the large roll-to-yaw ratios, he was not aware of a Dutch roll oscillation but only of the roll.

Although the damping was low compared to operational fighter-type aircraft, the pilot felt that it was adequate for the mission requirements of this type of vehicle.

Steady Sideslips

The control data obtained from steady-sideslip maneuvers are summarized in figure 12. The required rudder deflection per degree (radian) of sideslip agreed with the predictions; however, the aileron deflection required to maintain "wings-level" flight was less than predicted at high angles of attack. As a result, the apparent effectiveness of the ailerons relative to that of the rudders was greater than predicted. This does not necessarily mean that $C_{l\delta_a}$ is larger than predicted, inasmuch as several factors could be causing the discrepancy, as shown in the following relationships which were obtained from the equations of motion by setting the rolling and yawing velocities and accelerations to zero

$$\frac{\delta_r}{\beta} \approx \frac{C_{l\beta} C_{n\delta_a} - C_{n\beta} C_{l\delta_a}}{C_{n\delta_r} C_{l\delta_a} - C_{l\delta_r} C_{n\delta_a}}$$

$$\frac{\delta_a}{\beta} \approx \frac{C_{n\beta} C_{l\delta_r} - C_{l\beta} C_{n\delta_r}}{C_{n\delta_r} C_{l\delta_a} - C_{l\delta_r} C_{n\delta_a}}$$

Roll-Control Response

The pilot reported that the roll power which had been predicted to be marginal in simulator studies was satisfactory and that the elevons appeared to be considerably more effective in roll than predicted. This difference is not obvious from a comparison of the simulated and flight responses shown in figures 6(b) and 9. Approximately the same control deflections were used in both instances, and the maximum roll rates obtained were about the same.

Another measure of the roll rates obtainable from the ailerons is illustrated in figure 13, which presents the variation with angle of attack of $\frac{\omega_{\phi}^2}{\omega_{\psi}^2}$ obtained from the flight-measured derivatives. For comparison, the predicted variation is shown by the dashed curve. This parameter is the steady-state transfer function for the control of roll rate with aileron (see ref. 10). The approximate relationship is

$$\frac{\omega_{\phi}^2}{\omega_{\psi}^2} \approx \frac{N_{\beta} - L_{\beta} \frac{N_{\delta a}}{L_{\delta a}}}{N_{\beta} - \alpha_o L_{\beta}}$$

The departure from unity of this parameter is an indication of the coupling between roll and yaw. Values greater than unity indicate "favorable" yaw and a tendency for the pilot to induce oscillations. Values less than unity indicate adverse yaw and a tendency toward sluggishness in roll. The data shown in figure 13 indicate that the M2-F1 is sluggish in roll, as predicted.

In order to resolve the apparent discrepancy in the data regarding the roll effectiveness of the ailerons, the pilot "flew" the simulator with the flight-measured derivatives and the flight-vehicle control-system characteristics. With the simulator in this configuration, the pilot was satisfied that the flight vehicle was adequately represented. Although large roll rates could not be developed, the initial accelerations were considered satisfactory. Because of the limited operational requirements of this type of vehicle, there is probably no necessity for large roll rates. Thus, the pilot considered the roll-control system to be satisfactory.

Center Fin

The center fin was installed in an effort to provide the best possible handling qualities for the initial flights. It was subsequently shown to be unnecessary, so extensive tests on the center-fin configuration were not considered necessary. Before completing the flight program, however, one flight was made with the center fin reinstalled in order to resolve the previously mentioned discrepancy between the predicted vehicle stability and the pilot's earlier observations. Since this flight was made with a car tow, the data are limited. The pilot did report an apparent increase in stability, however, which confirmed the original predictions. One possible explanation for this change in the pilot's report is pilot experience, which is apparently an important consideration in evaluating the handling qualities of such an unconventional vehicle as the M2-F1.

DERIVATIVE ANALYSIS

Control Derivatives

The control derivatives were obtained from the initial response to rudder and aileron pulses, assuming that the contributions of all derivatives other than that from the control deflection were negligible. The following equations were used

$$C_{l_{\delta a}} = \frac{\dot{p}}{\delta_a} \left(\frac{I_X}{\bar{q}Sb} \right)$$

$$C_{n\delta_a} = \frac{\dot{r}}{\delta_a} \left(\frac{I_Z}{\bar{q}Sb} \right)$$

$$C_{Y\delta_a} = \frac{a_y}{\delta_a} \left(\frac{W}{\bar{q}S} \right)$$

$$C_{l\delta_r} = \frac{\dot{p}}{\delta_r} \left(\frac{I_X}{\bar{q}Sb} \right)$$

$$C_{n\delta_r} = \frac{\dot{r}}{\delta_r} \left(\frac{I_Z}{\bar{q}Sb} \right)$$

$$C_{Y\delta_r} = \frac{a_y}{\delta_r} \left(\frac{W}{\bar{q}S} \right)$$

The analog-matching technique (ref. 11) was also used to determine these derivatives. A typical time history of an aileron pulse with an analog match is shown in figure 14. The results from these two methods are shown in figures 15(a) and 15(b) where, in general, good agreement is indicated. The rolling moment due to aileron deflection agrees fairly well with the wind-tunnel values (fig. 15(a)); however, the flight data show more adverse yawing moments due to the ailerons. This adverse yawing moment would indicate a more severe problem in roll than had been predicted. The rudders are somewhat less effective than predicted; however, more rudder power than needed is available, and the pilot did not notice the difference in rudder effectiveness.

Stability Derivatives

The effective dihedral parameter $C_{l\beta}$, the directional-stability parameter $C_{n\beta}$, and the lateral-force parameter $C_{Y\beta}$ were obtained by using the following equations

$$C_{l\beta} = - \left(C_{l\delta_r} \frac{\delta_r}{\beta} + C_{l\delta_a} \frac{\delta_a}{\beta} \right) \quad (1)$$

$$C_{n\beta} = - \left(C_{n\delta_r} \frac{\delta_r}{\beta} + C_{n\delta_a} \frac{\delta_a}{\beta} \right) \quad (2)$$

$$C_{Y\beta} = - \frac{W}{\bar{q}S} \left(\frac{a_y}{\beta} \right) \quad (3)$$

The flight-measured control derivatives shown in figure 15 were used in equations (1) and (2), and the ratios $\frac{\delta_a}{\beta}$ and $\frac{\delta_r}{\beta}$ were obtained from steady

sideslips. In equation (3), the ratio $\frac{\dot{a}_y}{\beta}$ was obtained from the controls-fixed portion of the pulse data. The preceding parameters were also obtained by the analog-matching technique. The results from the two methods did not agree, as shown in figure 16. This discrepancy generally illustrates the difficulty of obtaining reliable stability derivatives from the data obtained in these tests. As expected, the agreement between flight and wind-tunnel data was also poor.

Other methods of obtaining these parameters were attempted, without success. One of the more commonly accepted methods of determining $C_{n\beta}$ is from the relationship: $\omega_\psi^2 \approx N_\beta - \alpha_0 I_\beta$. However, this expression can be used only when $N_\beta \gg \alpha_0 I_\beta$ or when α_0 and I_β are known. Because of the relatively large magnitude of $C_{l\beta}$ and the uncertainty in both $C_{l\beta}$ and the angle of inclination of the principal axis, it was not possible to determine $C_{n\beta}$ from the frequency. An attempt was also made to determine the derivatives by using a least-squares analysis; however, the scatter in the data was so great that the results were meaningless.

CONCLUDING REMARKS

By conventional standards for evaluating piloted fighter-type aircraft, the lateral-directional handling qualities of the M2-F1 lifting-body vehicle determined from this flight investigation would be considered marginal. The vehicle is sluggish in roll and lightly damped in the Dutch roll mode. Although the roll acceleration is acceptable, the ailerons produce adverse yaw, which severely limits the roll rates attainable. The M2-F1 was also found to be extremely sensitive to rough air, because of the large dihedral effect. However, the mission requirements for this type of vehicle do not require high maneuverability, and in calm air the pilots considered the lateral-directional handling qualities of the vehicle to be adequate.

Pilot experience was found to be a significant factor in evaluating the handling qualities of the M2-F1. Because it is an unconventional vehicle that had not been flown previously, there was some uncertainty about the flying qualities during the first flights. As a result, it was not surprising that the pilot ratings improved considerably with flight experience.

Although towing the M2-F1 was an operational problem peculiar to this investigation, and will not be a problem associated with future reentry vehicles, an interesting sidelight was the vehicle's characteristics on tow. Unlike most vehicles, which are less stable on tow than in free flight, the M2-F1 was predicted to be and was more stable when being towed.

Flight Research Center,
National Aeronautics and Space Administration,
Edwards, Calif., July 1, 1965.

REFERENCES

1. Horton, Victor W.; Eldredge, Richard C.; and Klein, Richard E.: Flight-Determined Low-Speed Lift and Drag Characteristics of the Lightweight M2-F1 Lifting Body. NASA TN D-3021, 1965.
2. Mechtly, E. A.: The International System of Units - Physical Constants and Conversion Factors. NASA SP-7012, 1964.
3. Dennis, David H.; and Edwards, George G.: The Aerodynamic Characteristics of Some Lifting Bodies. NASA TM X-376, 1960.
4. Kenyon, George C.: The Lateral and Directional Aerodynamic Characteristics of a Re-entry Configuration Based on a Blunt 13° Half Cone at Mach Numbers to 0.90. NASA TM X-583, 1961.
5. Kenyon, George C.; and Edwards, George G.: A Preliminary Investigation of Modified Blunt 13° Half-Cone Re-entry Configurations at Subsonic Speeds. NASA TM X-501, 1961.
6. Kenyon, George C.; and Sutton, Fred B.: The Longitudinal Aerodynamic Characteristics of a Re-entry Configuration Based on a Blunt 13° Half-Cone at Mach Numbers to 0.92. NASA TM X-571, 1961.
7. Rakich, John V.: Supersonic Aerodynamic Performance and Static-Stability Characteristics of Two Blunt-Nosed, Modified 13° Half-Cone Configurations. NASA TM X-375, 1960.
8. Rakich, John V.: Aerodynamic Performance and Static-Stability Characteristics of a Blunt-Nosed, Boattailed, 13° Half-Cone at Mach Numbers From 0.6 to 5.0. NASA TM X-570, 1961.
9. Hassell, James L., Jr.; and Ware, George M.: Investigation of the Low-Subsonic Stability and Control Characteristics of a 0.34-Scale Free-Flying Model of a Modified Half-Cone Reentry Vehicle. NASA TM X-665, 1962.
10. Taylor, Lawrence W., Jr.; and Day, Richard E.: Flight Controllability Limits and Related Human Transfer Functions as Determined From Simulator and Flight Tests. NASA TN D-746, 1961.
11. Yancey, Roxanah B.: Flight Measurements of Stability and Control Derivatives of the X-15 Research Airplane to a Mach Number of 6.02 and an Angle of Attack of 25° . NASA TN D-2532, 1964.

TABLE I

PHYSICAL CHARACTERISTICS OF THE M2-F1 LIFTING-BODY VEHICLE

| | |
|---|-----------------------------|
| Body - | |
| Length, ft (m) | 20 (6.1) |
| Planform area, ft ² (m ²) | 139 (12.9) |
| Span, ft (m) | 9.54 (2.9) |
| Weight, lb (kg) | 1182 (536) |
| Elevons - | |
| Area, ft ² (m ²) | 6.51 (0.6) |
| Span, ft (m) | 2.33 (0.7) |
| Root chord, ft (m) | 3.83 (1.2) |
| Deflection, deg (rad) | -22 (-0.38) to 9 (0.16) |
| Flaps - | |
| Area, ft ² (m ²) | 8.60 (0.8) |
| Span, ft (m) | 4.38 (1.3) |
| Chord, ft (m) | 2.19 (0.7) |
| Deflection, deg (rad) | -19.5 (-0.34) to -5 (-0.09) |
| Rudders - | |
| Area, ft ² (m ²) | 5.34 (0.5) |
| Span, ft (m) | 4.27 (1.3) |
| Chord, ft (m) | 1.25 (0.4) |
| Deflection, deg (rad) | ±4.5 (±0.08) |
| Moments of inertia (calculated for 840-lb vehicle (381 kg)) - | |
| I _X , slug-ft ² (kg-m ²) | 200 (890) |
| I _Y , slug-ft ² (kg-m ²) | 868 (3861) |
| I _Z , slug-ft ² (kg-m ²) | 920 (4092) |
| I _{XZ} , slug-ft ² (kg-m ²) | 0 (0) |
| Moments of inertia (estimated for 1182-lb vehicle (536 kg)) - | |
| I _X , slug-ft ² (kg-m ²) | 225 (1001) |
| I _Y , slug-ft ² (kg-m ²) | 1100 (4893) |
| I _Z , slug-ft ² (kg-m ²) | 1125 (5004) |
| I _{XZ} , slug-ft ² (kg-m ²) | -25 (-111) |

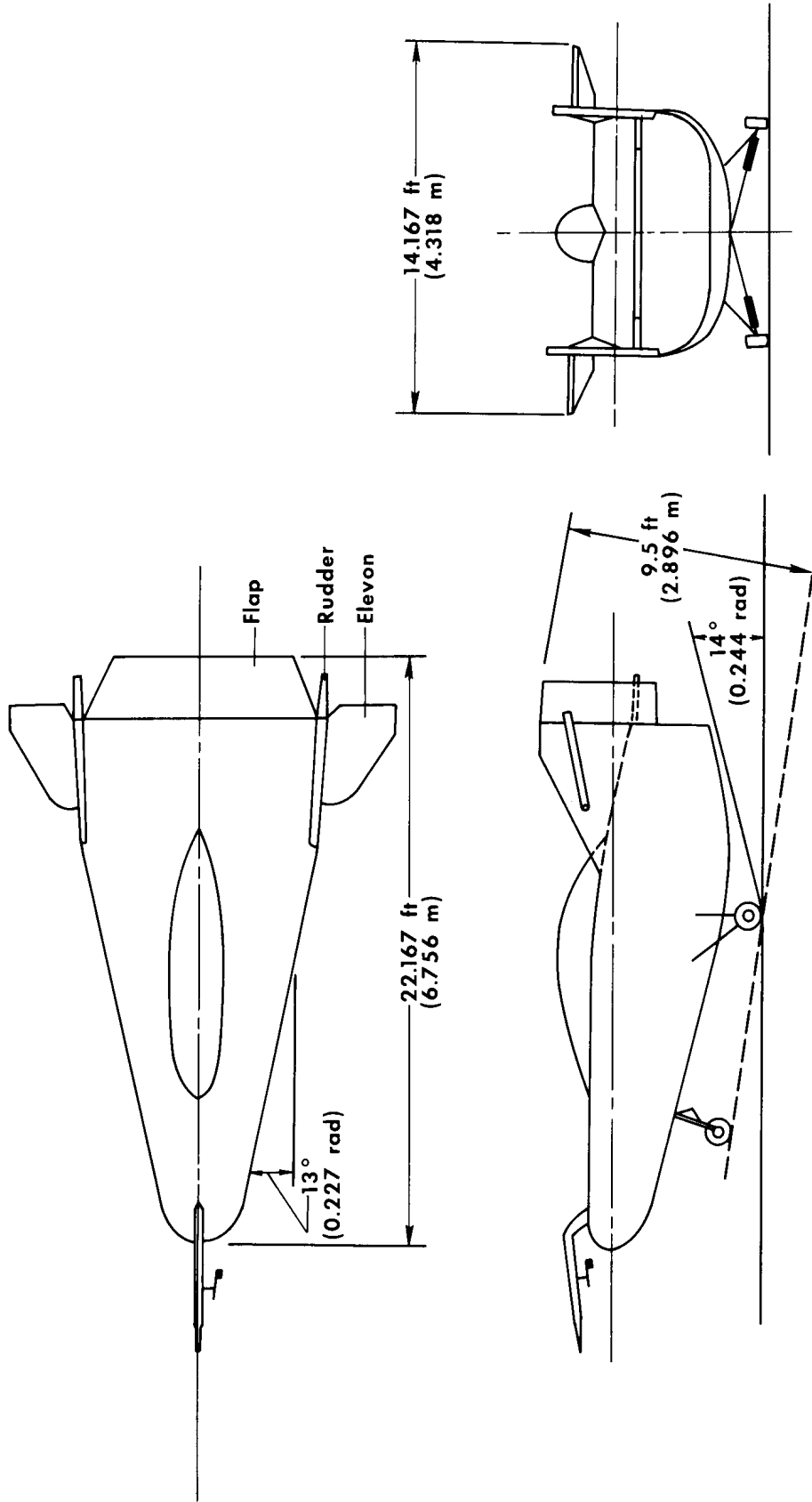
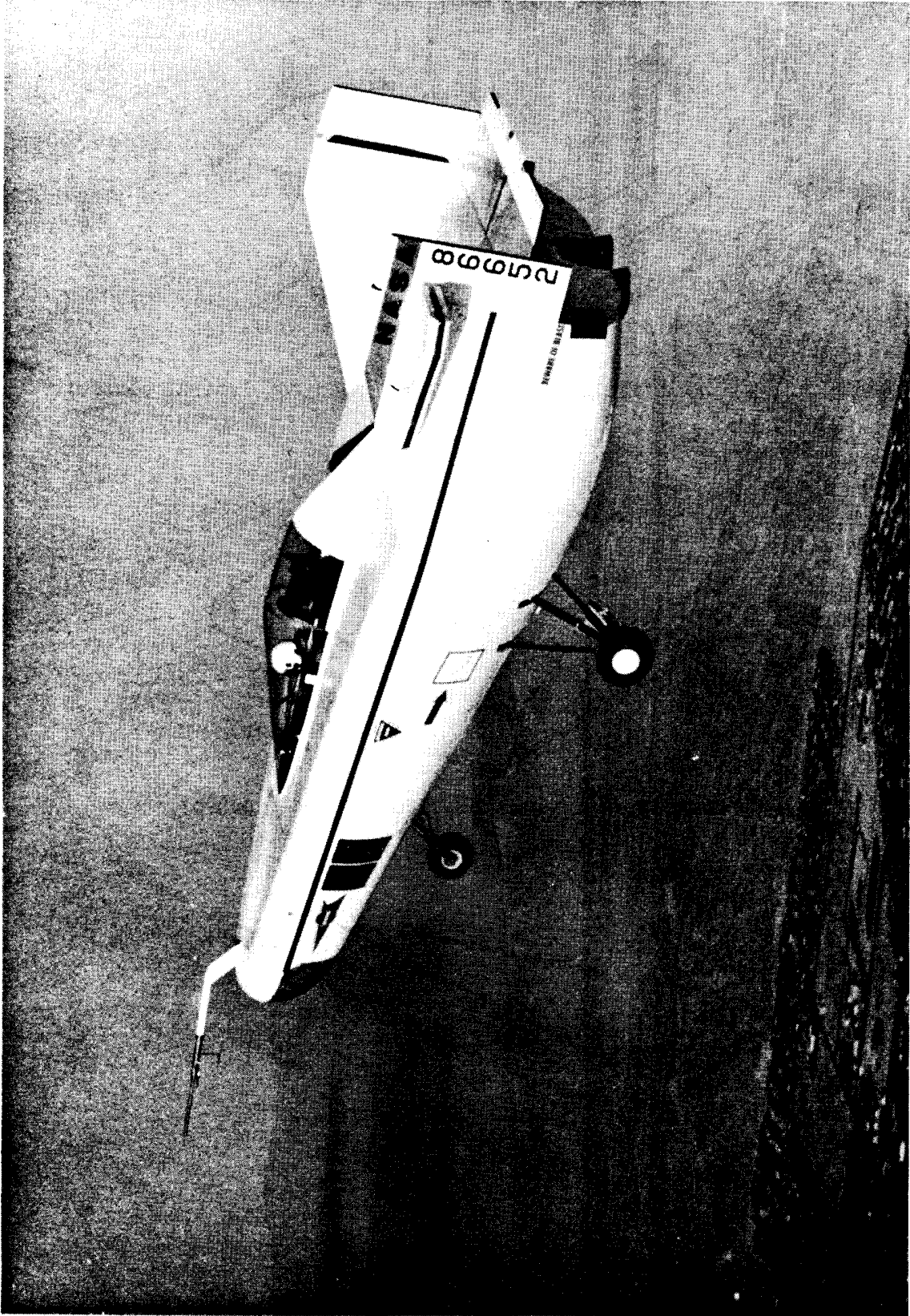
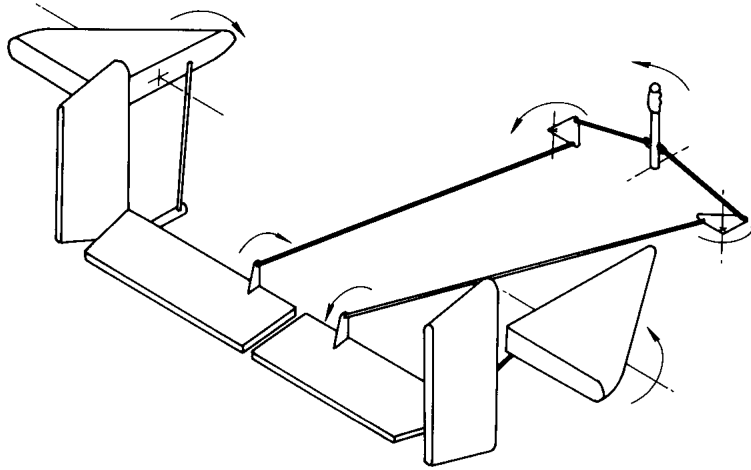


Figure 1.- Three-view drawing of M2-F1.

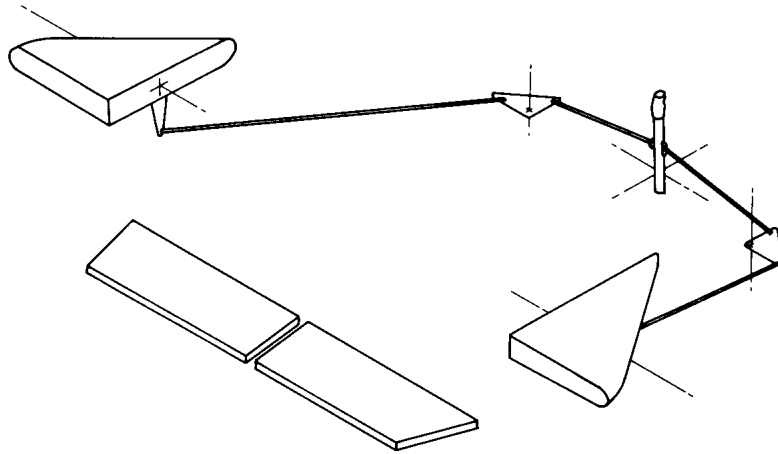


ECN-407

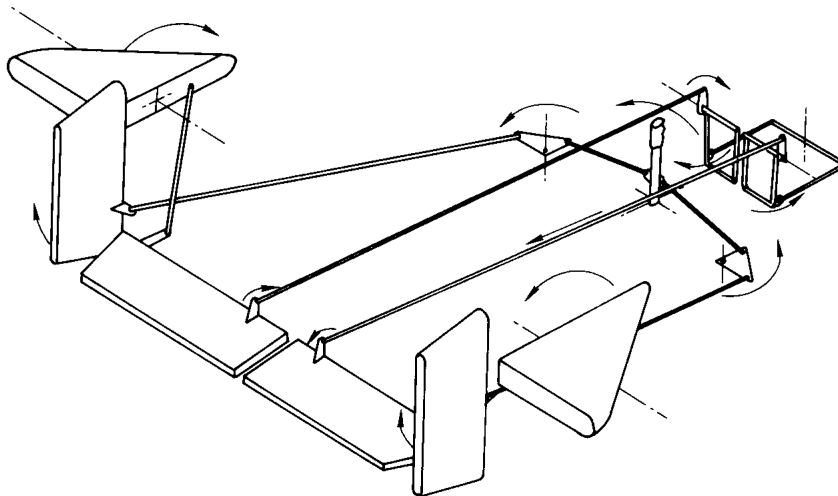
Figure 2.- Photograph of M2-Fl.



(a) Both outboard and trailing-edge surfaces used for lateral control.

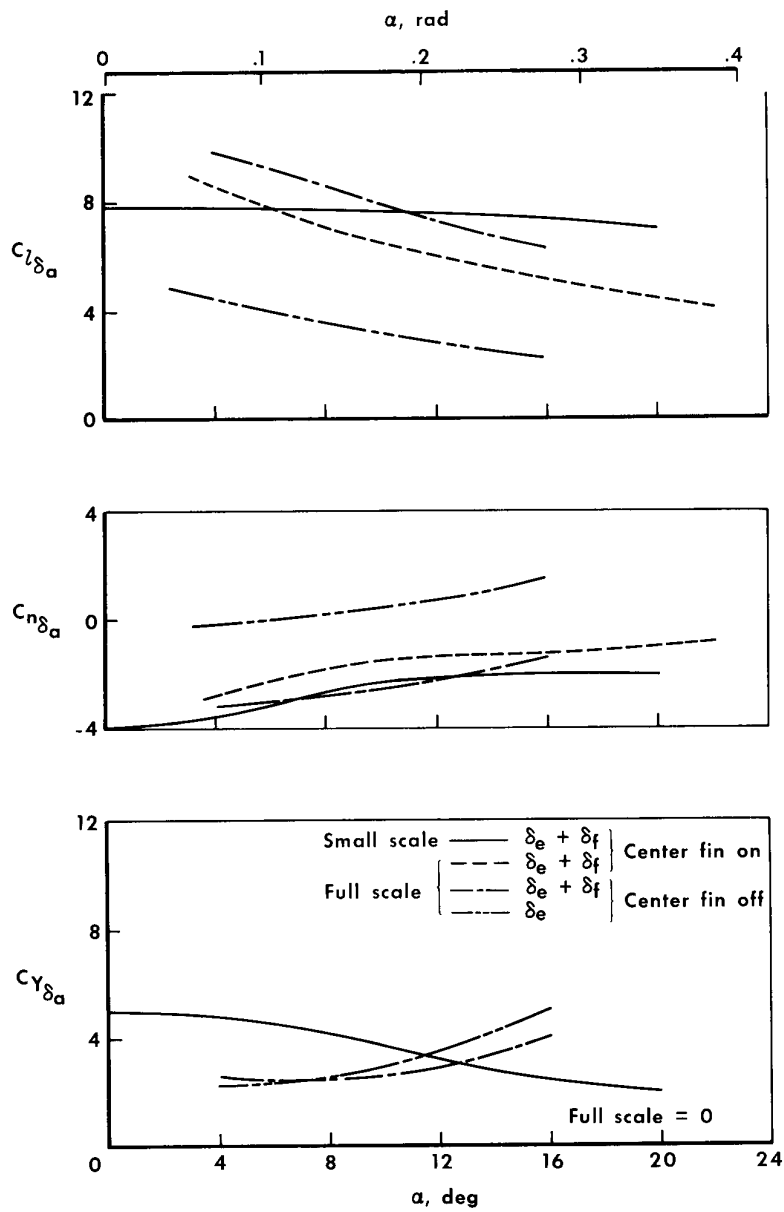


(b) Outboard surfaces only used for lateral control.



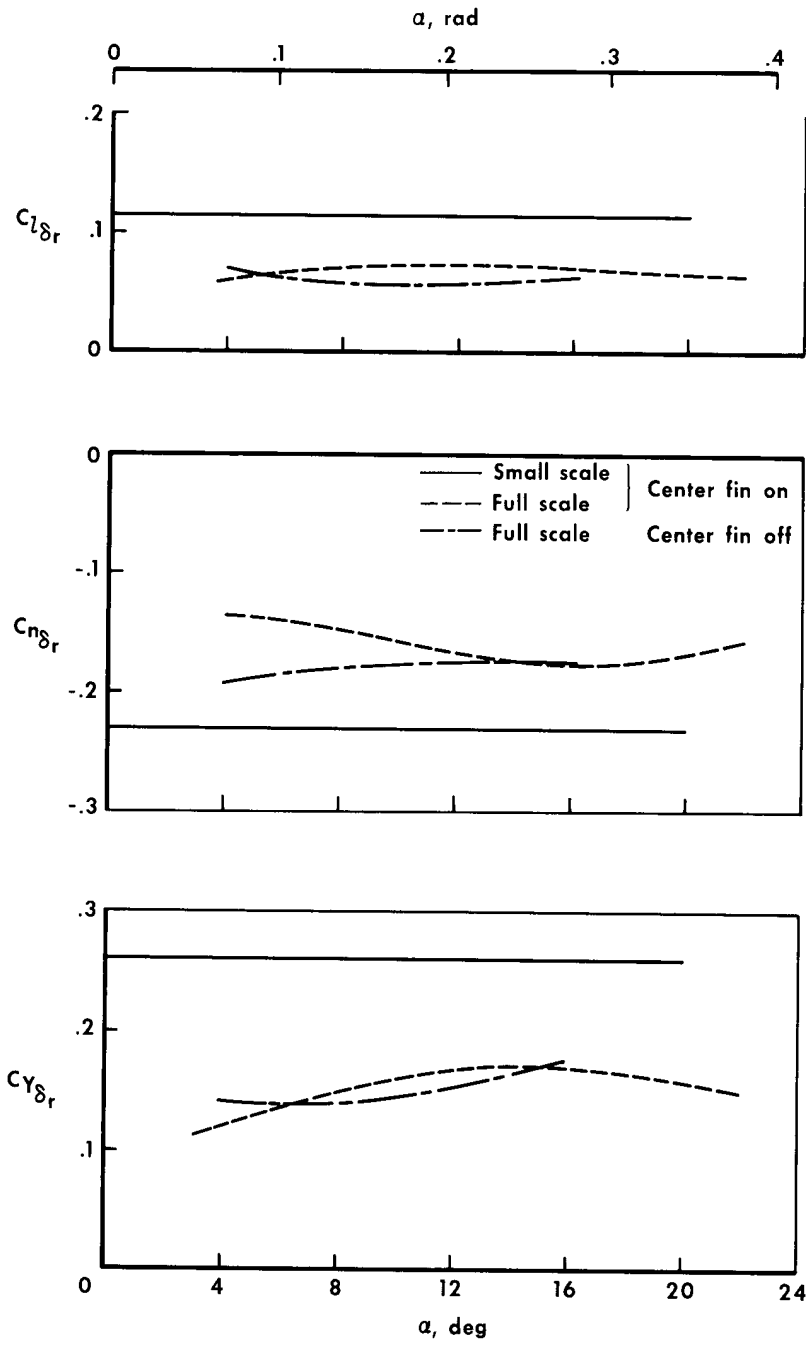
(c) Rudders used for lateral control.

Figure 3.- Schematic drawings of three proposed lateral-control systems.



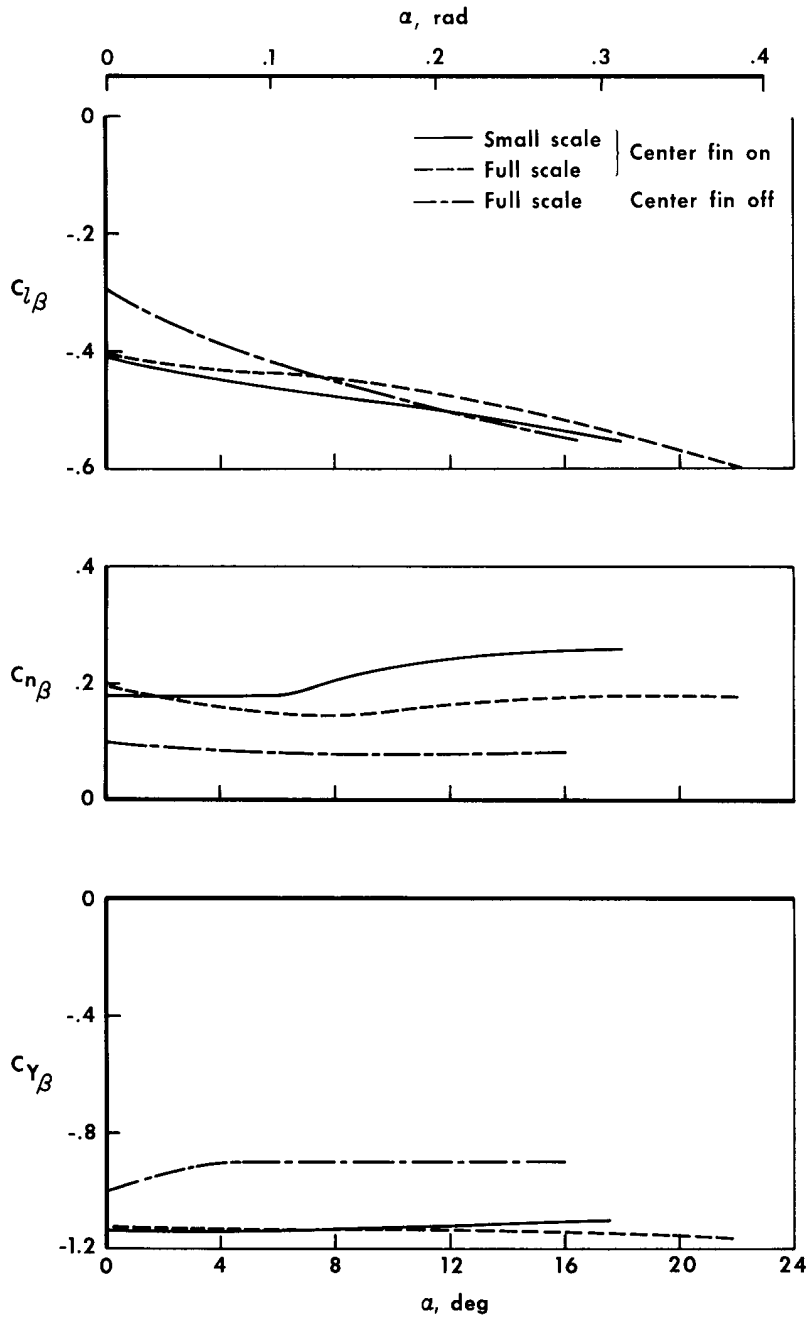
(a) Aileron derivatives.

Figure 4.- Comparison of full-scale tunnel data with small-scale tunnel data for the M2-F1 configuration.



(b) Rudder derivatives.

Figure 4.- Continued.



(c) Lateral-directional-stability derivatives.

Figure 4.- Concluded.

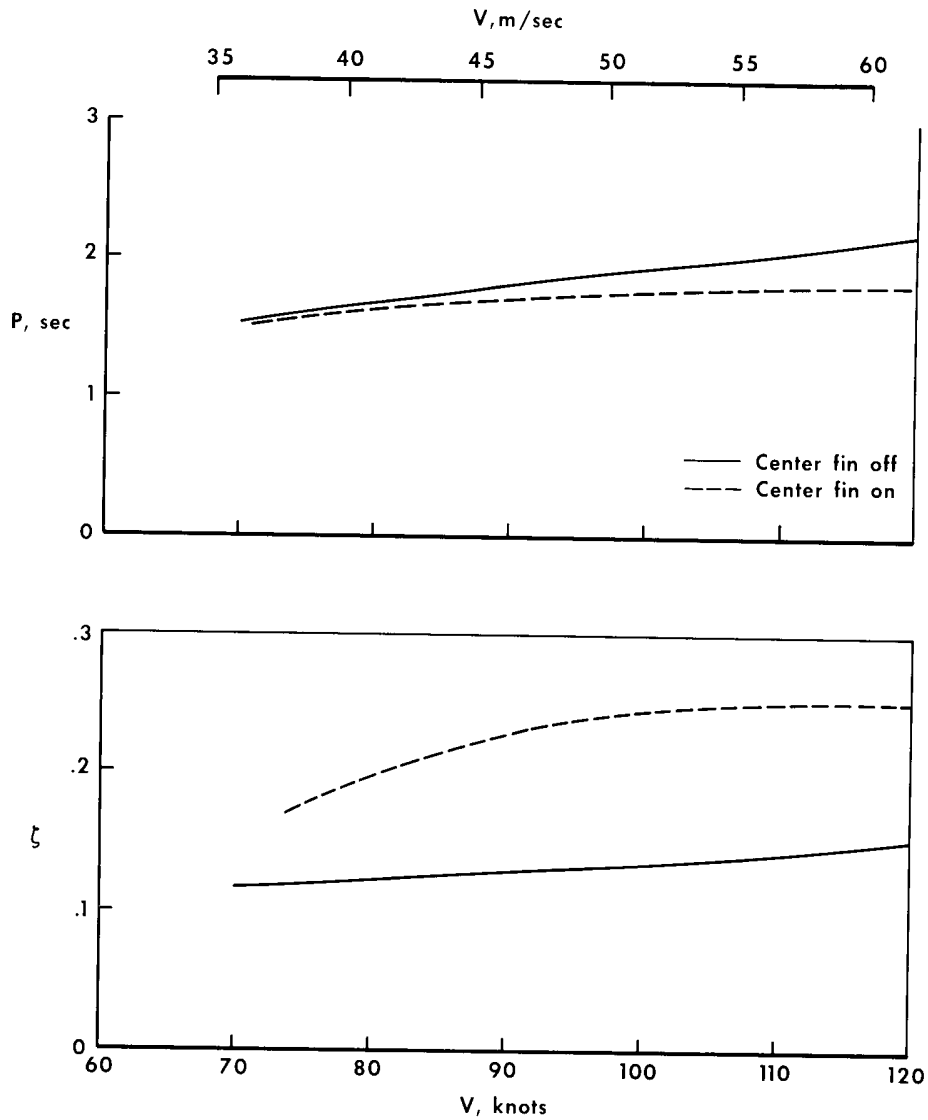
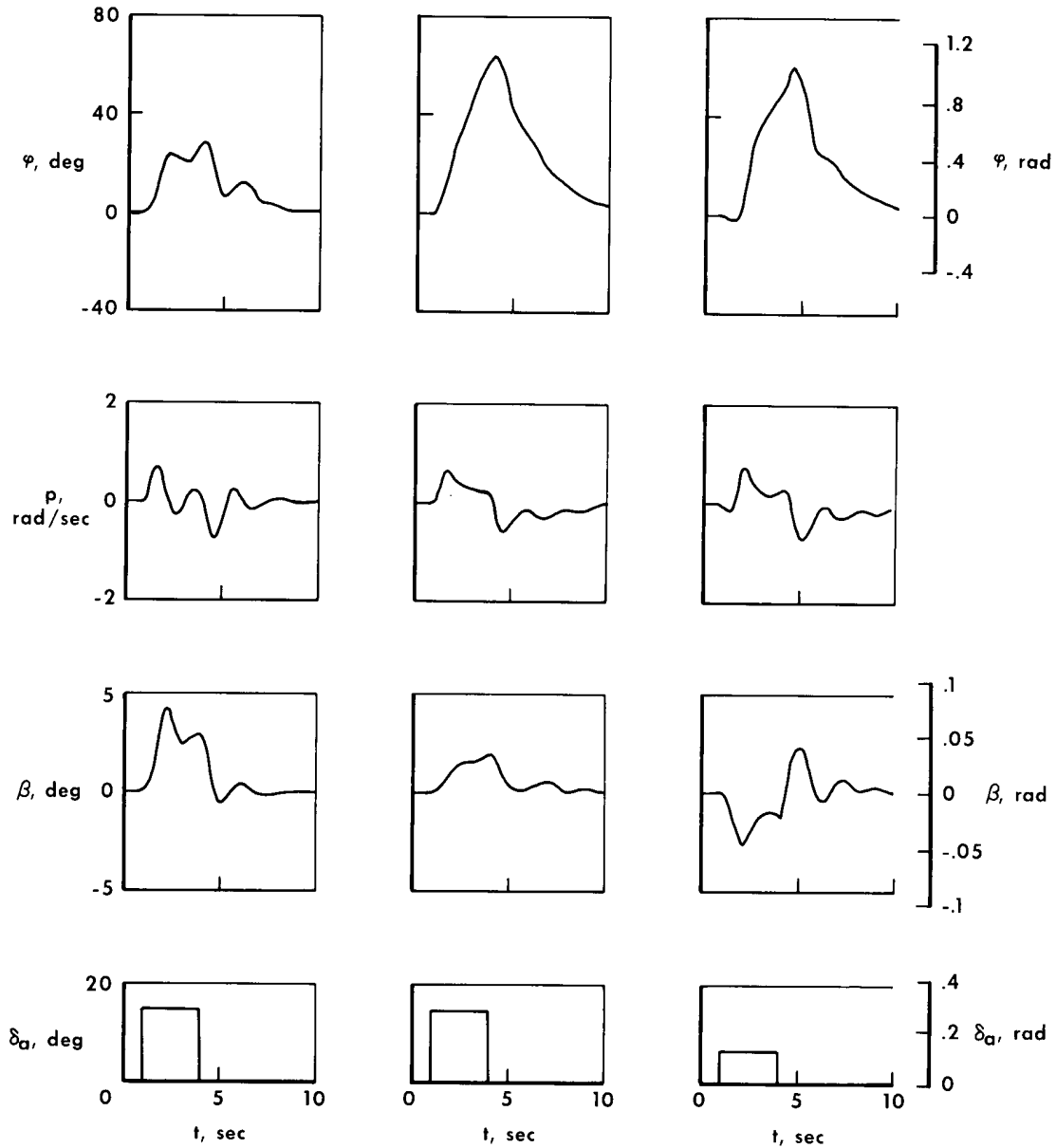


Figure 5.- Effect of center fin on period and damping of M2-F1.



(a) Both outboard and trailing edge surfaces used for lateral control.

(b) Outboard surfaces only used for lateral control.

(c) Rudders used for lateral control.

Figure 6.- Time histories of three lateral-control step inputs obtained from the simulator. $\alpha = 0^\circ$; $V = 100$ knots (51.4 meters/second); $\bar{q} = 31.5$ lb/ft² (1508 N/m²).

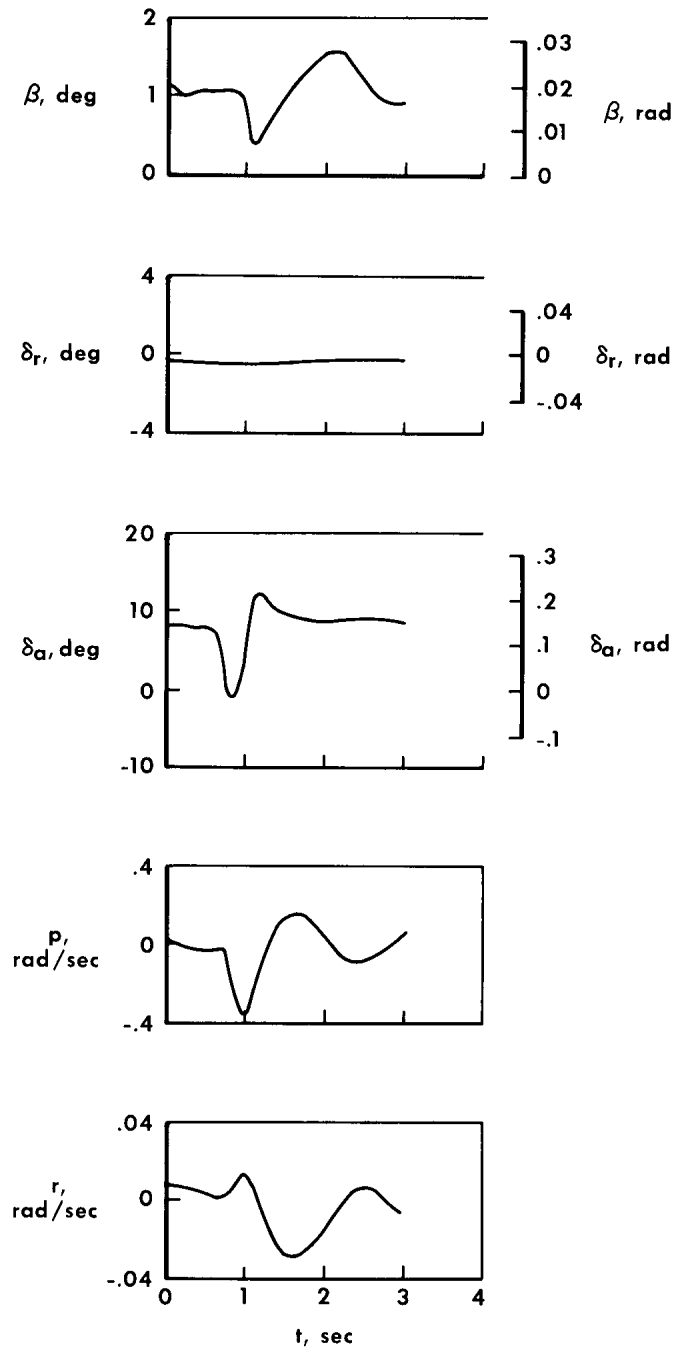


Figure 7.— Time history of an aileron pulse. $\alpha \approx 2^\circ$ (0.035 rad);
 $V \approx 95$ knots (49 meters/second); $\bar{q} \approx 30.2$ lb/ft² (1446 N/m²).

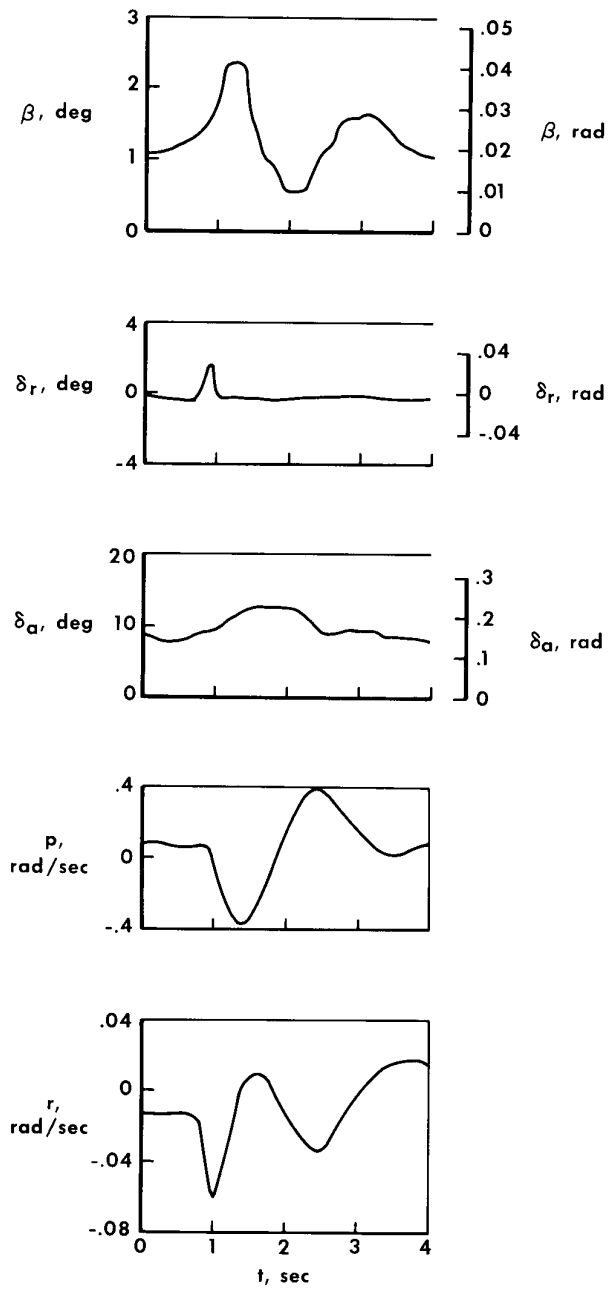


Figure 8.- Time history of a rudder pulse. $\alpha \approx 2^\circ$ (0.035 rad);
 $V \approx 95$ knots (49 meters/second); $\bar{q} \approx 30.2$ lb/ft² (1446 N/m²).

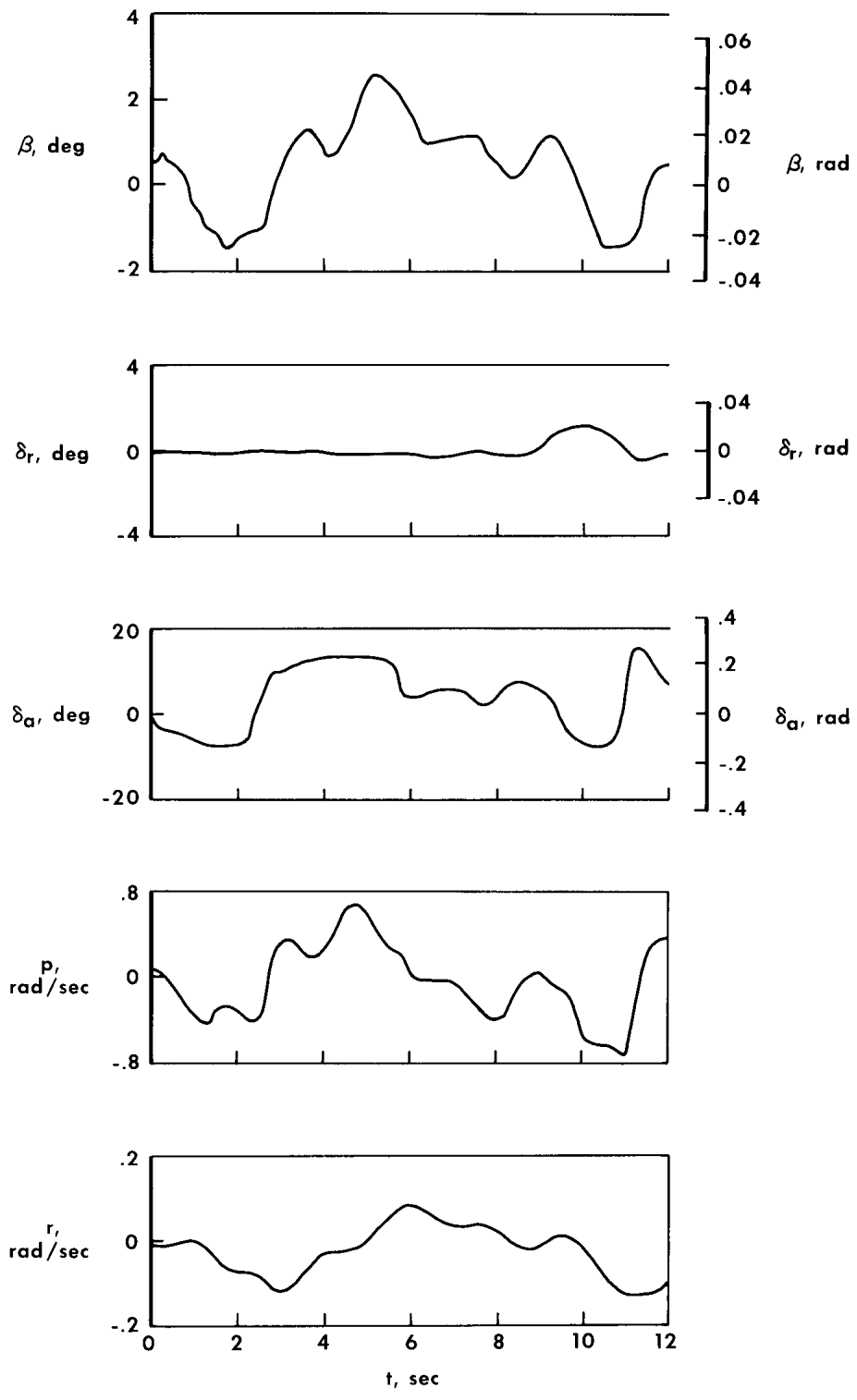


Figure 9.— Time history of a rudder-fixed aileron roll. $\alpha \approx 2^\circ$ (0.035 rad); $V \approx 95$ knots (49 meters/second); $\bar{q} \approx 30.2$ lb/ft² (1446 N/m²).

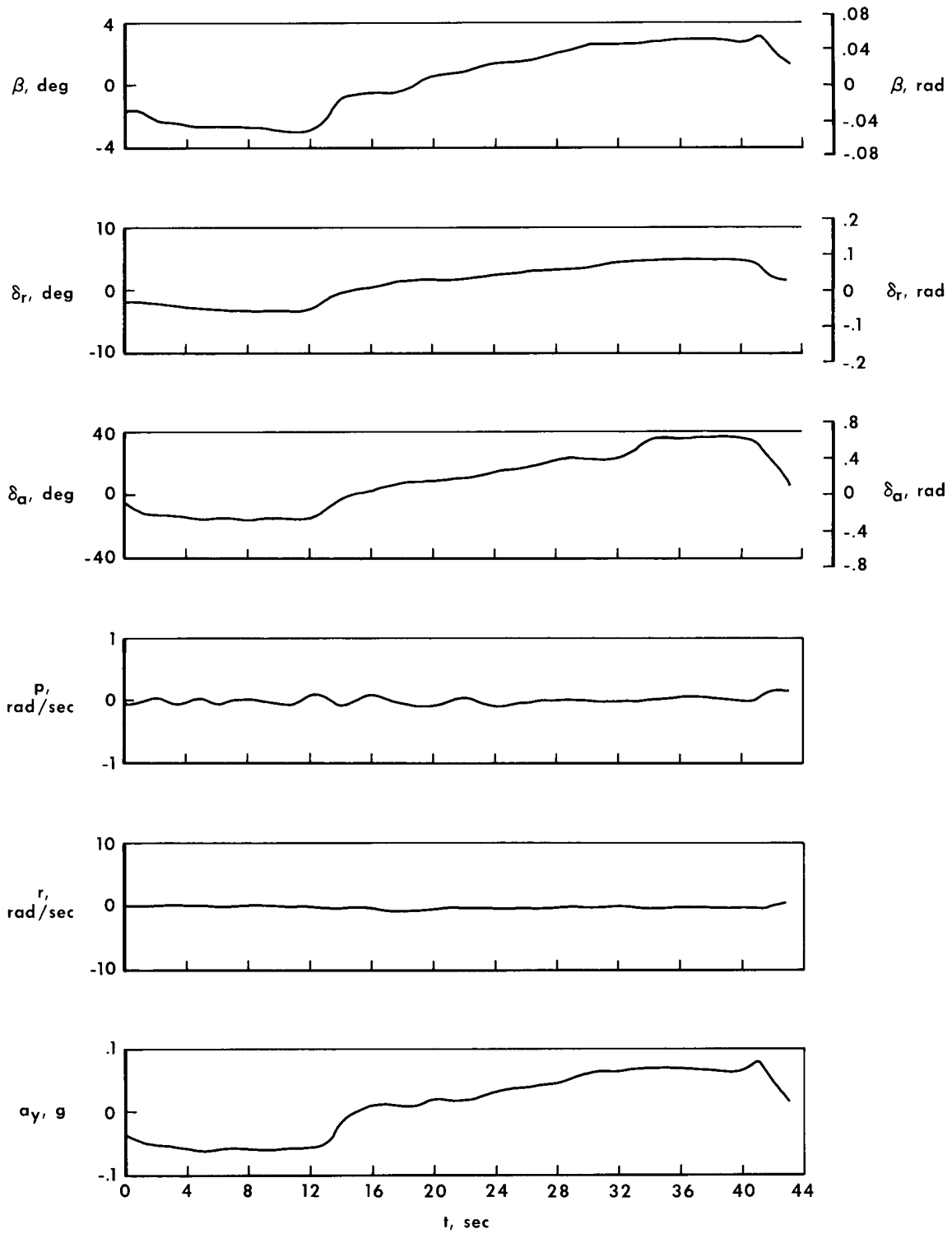


Figure 10.— Time history of a steady-state sideslip. $\alpha \approx 12^\circ$ (0.210 rad); $V \approx 80$ knots (41 meters/second); $\bar{q} \approx 17.3$ lb/ft² (828 N/m²).

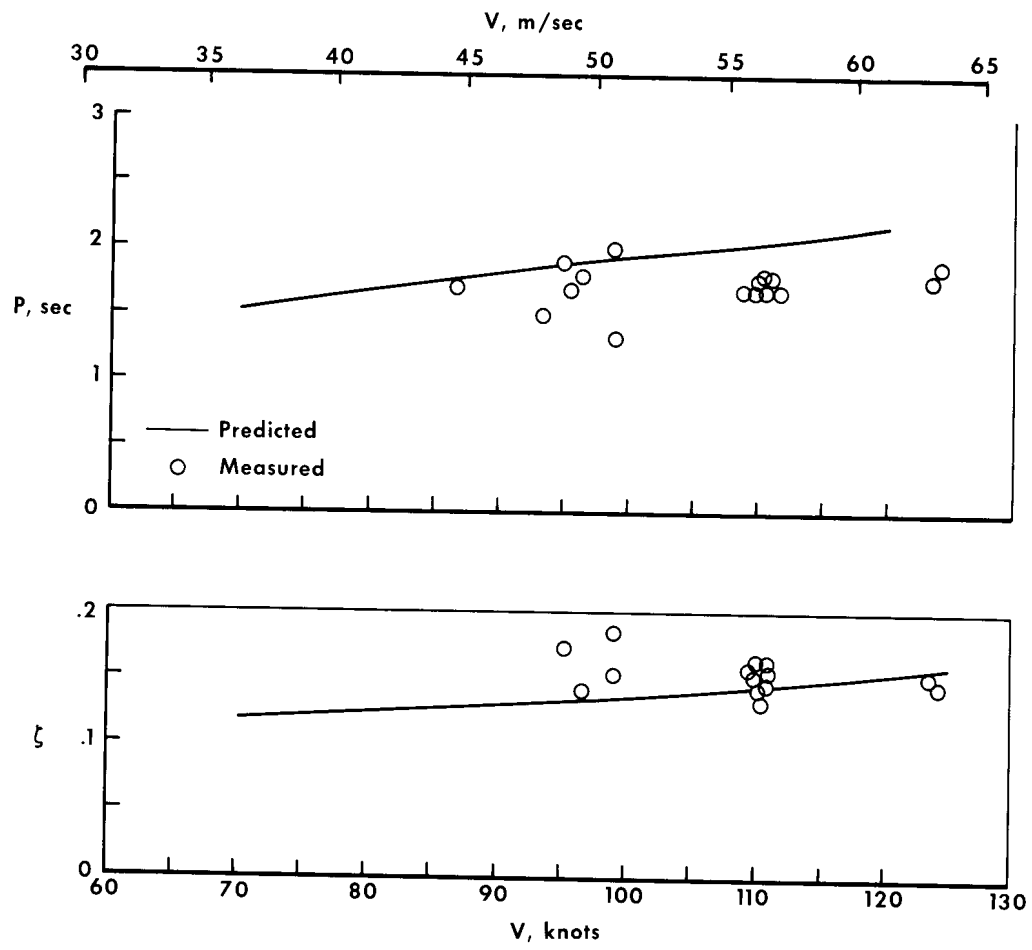


Figure 11.— Variation of period and damping ratio of M2-F1 with airspeed.

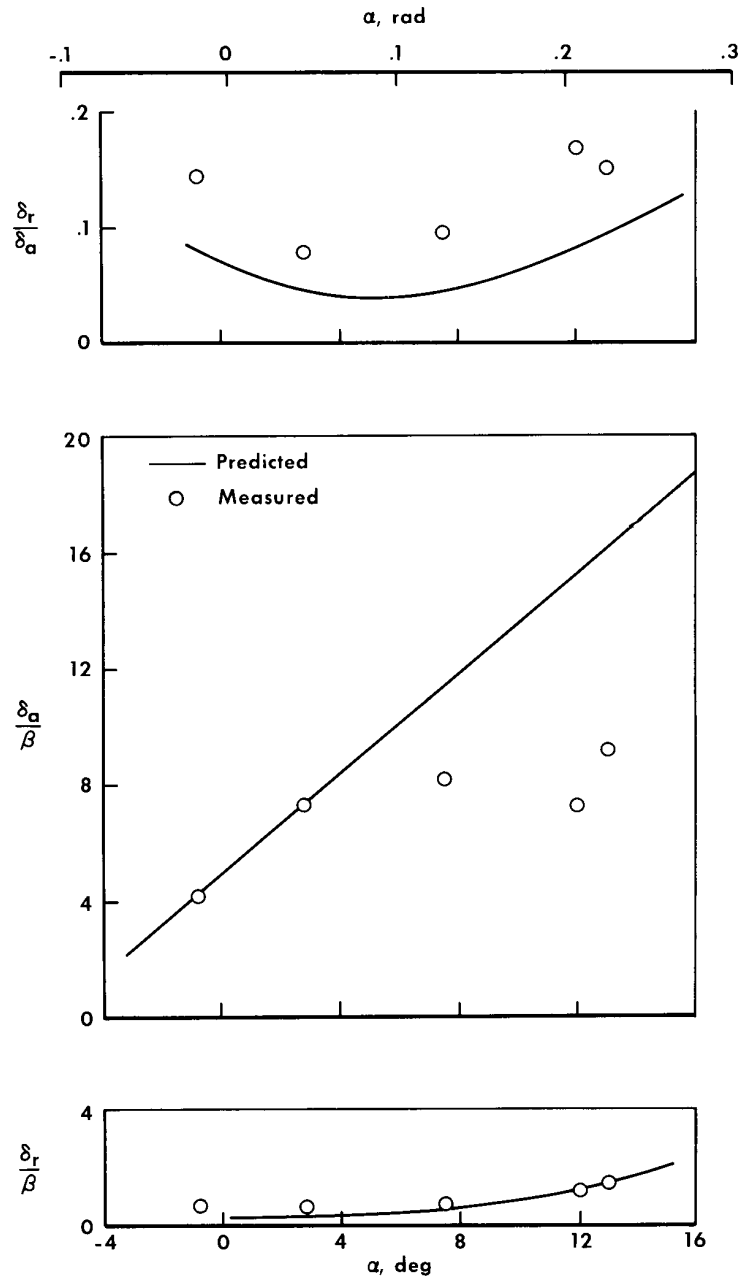


Figure 12.- Variation of static lateral-stability parameters with angle of attack as determined from steady sideslips.

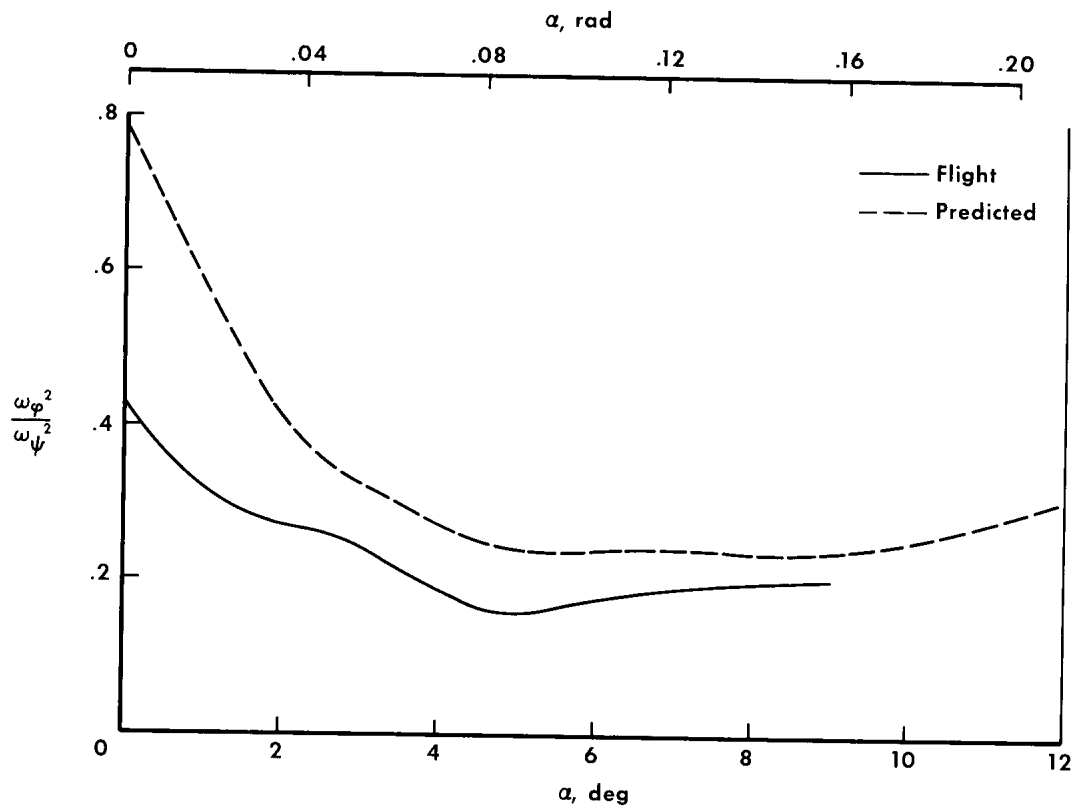


Figure 13.- Variation with angle of attack of roll numerator to Dutch roll frequency ratio.

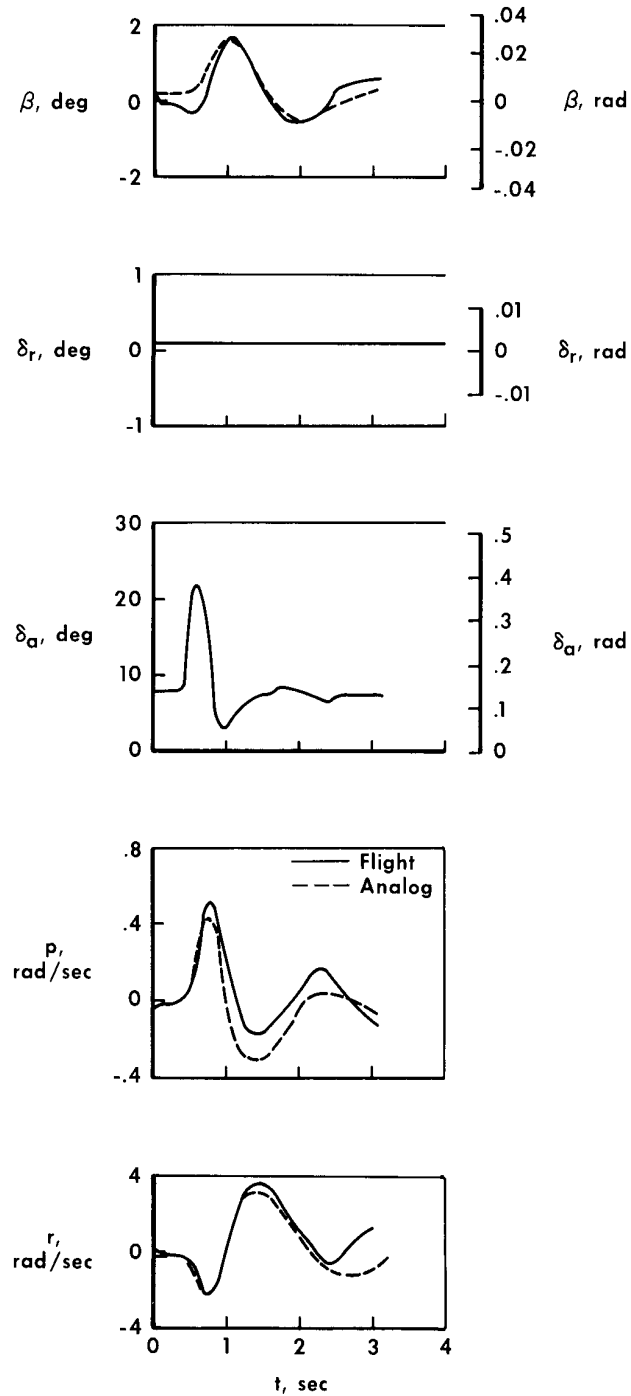
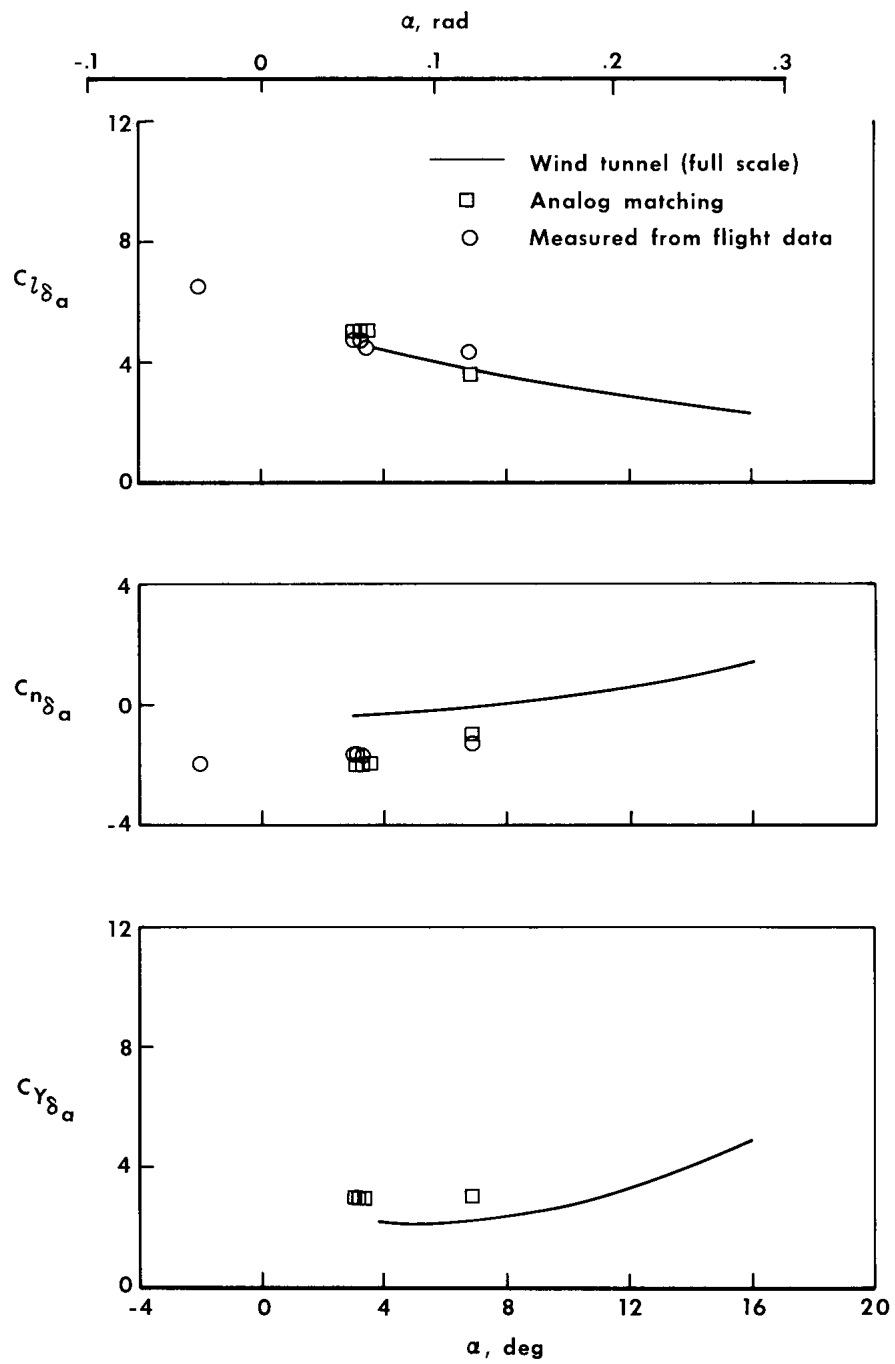
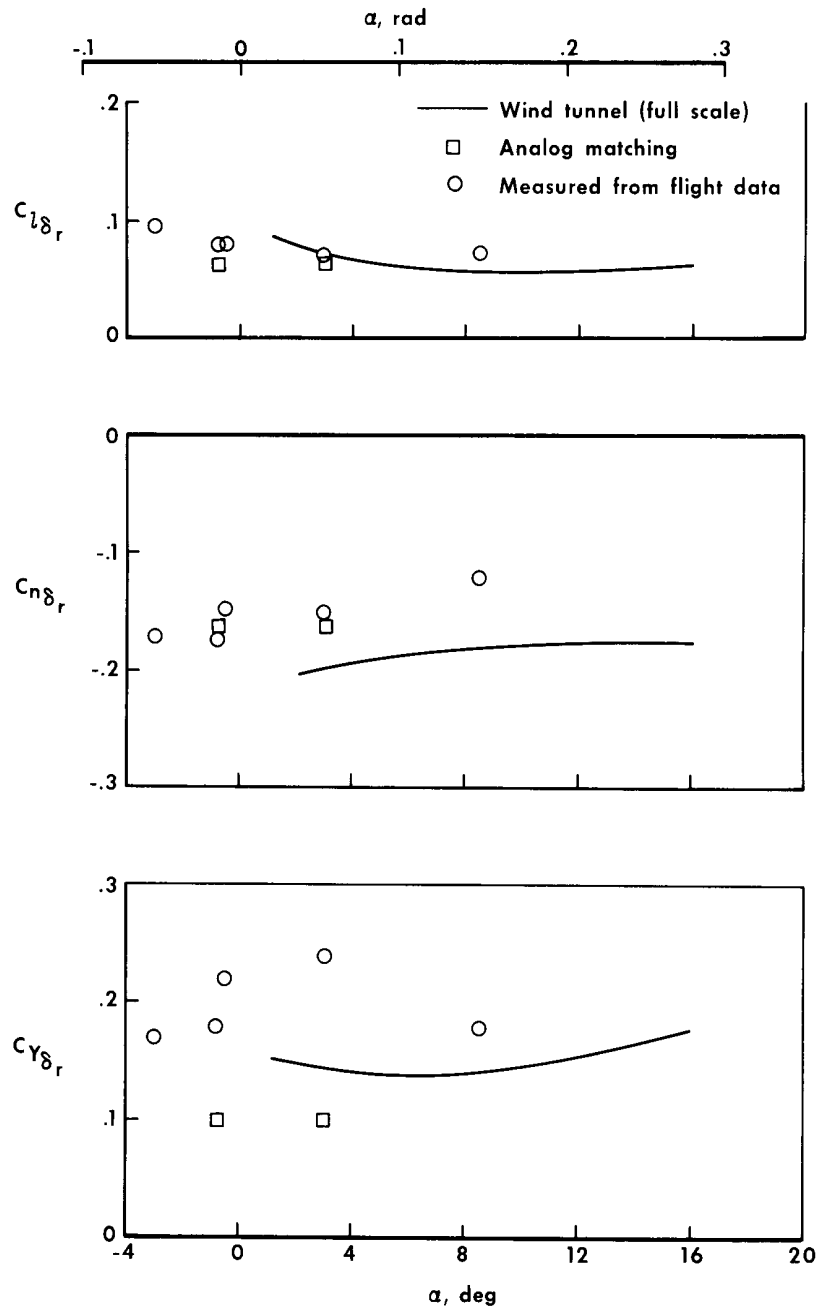


Figure 14.- Typical time history of an aileron pulse with an analog match.
 $\alpha \approx 7^\circ$ (0.150 rad); $V \approx 89$ knots (46 meters/second); $\bar{q} \approx 27$ lb/ft²
(1293 N/m²).



(a) Aileron derivatives.

Figure 15.— Variation of lateral-control derivatives with angle of attack.



(b) Rudder derivatives.

Figure 15.- Concluded.

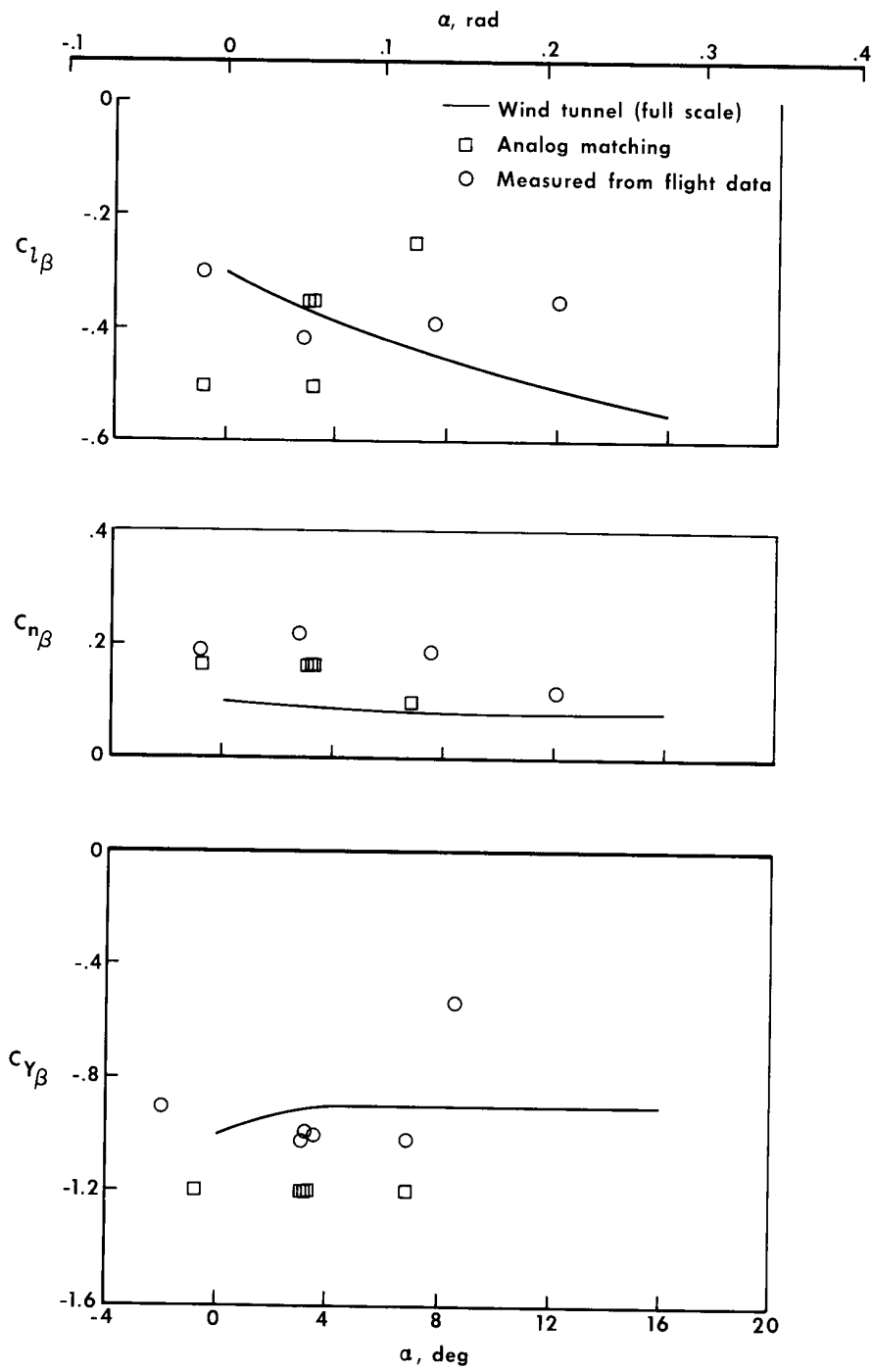


Figure 16.- Variation of lateral-directional-stability derivatives with angle of attack.